Journal of Catalysis 260 (2008) 351–357

Contents lists available at ScienceDirect

Journal of Catalysis

www.elsevier.com/locate/jcat

Kinetics of CO oxidation catalyzed by highly dispersed CeO_2-supported gold

Veronica Aguilar-Guerrero, Bruce C. Gates *

Department of Chemical Engineering and Materials Science, University of California, Davis, CA 95616, USA

ARTICLE INFO

Article history:
Received 16 August 2008
Revised 17 September 2008
Accepted 17 September 2008
Available online 31 October 2008

Keywords:
Gold
CO oxidation kinetics
Gold clusters

ABSTRACT

CeO_2-supported gold synthesized from $Au(CH_3)_2(acac)$ (acac: acetylacetonate) catalyzed CO oxidation at 353 K, with a turnover frequency TOF of 6.3×10^{-3} molecules of CO (Au atom s)$^{-1}$ at CO and O_2 partial pressures of 1.0 kPa; the apparent activation energy was 138 ± 2 kJ mol^{-1}. The activity increased as the catalyst functioned in a flow reactor, and after 48 h on stream, the TOF at 298 K and the aforementioned CO and O_2 partial pressures was $(5.6 \pm 0.2) \times 10^{-2}$ molecules of CO (Au atom s)$^{-1}$. X-ray absorption spectra, reported separately, showed that the catalyst structure changed during operation, as the mononuclear cationic species present initially formed clusters consisting on average of roughly 15 Au atoms each. The gold clusters were more active for CO oxidation catalysis than the mononuclear gold species. Reaction orders of CO oxidation catalyzed by the sample containing the clusters at 303 K were found to be 0.19 in CO, 0.18 in O_2, and −0.4 in CO_2. The apparent activation energy characterizing the catalyst containing the clusters was found to be only about one-third of that characterizing the catalyst incorporating the mononuclear cationic gold.

1. Introduction

Extensive research on catalysis by supported gold has been reported since the pioneering discoveries by Hutchings [1] and Haruta [2] demonstrating high activities of highly dispersed gold. CO oxidation and the water–gas shift [3] are among the most widely investigated of the reactions catalyzed by supported gold; most of the work has focused on these reactions, especially the former [4], because they apparently offer the advantages of simplicity conferred by small reactant molecules and the value of CO as a sensitive probe of surface sites [5].

Notwithstanding the extensive research on CO oxidation catalyzed by supported gold, the mechanism(s) of the reaction and the catalytically active species remain under debate. There is a lack of consensus regarding the oxidation states of gold in the catalysts and the effects of gold oxidation state on catalytic activity, but there appears to be a consensus that extremely high gold dispersion favors catalytic activity and that the activity depends on the gold cluster size [6], although data characterizing the performance of the smallest gold clusters are lacking.

A number of reports include values of turnover frequencies (TOFs) [7], but reports of kinetics of gold-catalyzed CO oxidation are few and largely incomplete. The most thorough such investigations were reported by the group of Haruta [7], for Au/TiO_2, and by Lin et al. [8], for Au/TiO_2 and Au/SiO_2. Typical orders of reaction in CO and in O_2 are in the range of 0.1–0.6; there are a few reports of the influence of CO_2 on the rate [9–11].

Although many supported gold catalysts are so active that they can be investigated at temperatures below room temperature, measurements of CO oxidation kinetics have been hindered by such complications as rapid catalyst deactivation. Characterization of the deactivation is lacking for most supported gold catalysts, and often it is difficult to determine whether reported conversions or reaction rates characterize fresh or deactivated catalysts. Denkwitz et al. [12] investigated catalyst deactivation during CO oxidation catalysis in flow reactor and found that the rate of deactivation was lower when the reaction proceeded in an O_2-rich atmosphere. Suggested causes of catalyst deactivation include sintering of the gold, with loss of catalyst surface area [13]; formation of deposits on the catalyst surface, including carbonate-like species [9]; and changes in the gold oxidation state [14]. The performance of supported gold catalysts depends sensitively on the presence of water in the feed stream [15], and only Haruta et al. [15] demonstrated the capability of varying the water partial pressure sufficiently finely to allow thorough quantitative assessment of the effects of water. Data characterizing Au/TiO_2, Au/Al_2O_3, and Au/SiO_2 indicate that moisture concentration influences the catalytic activity at concentrations ranging from 0.1 to 6000 ppm.

Our goal in the present work was to investigate CO oxidation in the presence of catalysts incorporating site-isolated cationic gold complexes on a support and to compare the results with those determined with a catalyst consisting of small gold clusters on the same support. We summarize data demonstrating the following:

* Corresponding author.
E-mail address: bcgates@ucdavis.edu (B.C. Gates).

0021-9517/$ – see front matter
doi:10.1016/j.jcat.2008.09.012

(1) synthesis of CeO_2-supported catalysts consisting initially of single-gold-atom (mononuclear) species on the support;
(2) catalytic activity of the mononuclear gold species;
(3) formation of clusters of roughly 15 Au atoms each, on average, from the mononuclear species during CO oxidation catalysis in a flow reactor, accompanied by an increase in the catalytic activity—a result that demonstrates that clusters consisting of only a few Au atoms are more active than the mononuclear species;
(4) a comparison of the apparent activation energies of the reactions catalyzed by the mononuclear and cluster catalysts, demonstrating the contrast between them; and
(5) quantitative kinetics describing the reaction catalyzed by the supported gold clusters.

CeO_2 was chosen as the support because some of the most active gold catalysts are supported on CeO_2 [13]. Guzman et al. [16,17] determined Raman spectra indicating the role of this support in activating oxygen for the CO oxidation reaction.

$Au(CH_3)_2(acac)$ (acac: the bidentate ligand acetylacetonate, $CH_3COCHCOCH_3$) was chosen as the catalyst precursor because it is highly reactive with the support, being converted into supported mononuclear gold species [18], and because it lacks anions, such as chloride, that complicate structure determination and influence the catalyst performance [8]. Supported gold samples synthesized under mild, controlled conditions from this precursor offer the advantages of simple, nearly molecular structures, which, on mild treatment, may give extremely small clusters of gold [14,18,19].

2. Experimental methods

2.1. Synthesis of Au/CeO_2

Catalyst samples were synthesized and handled with the exclusion of moisture and air using a double-manifold Schlenk vacuum line and a glove box purged with argon that was recirculated through traps containing supported copper and zeolite 4A for removal of O_2 and moisture, respectively. Samples containing 1.0 wt% Au were synthesized from $Au(CH_3)_2(acac)$ (Strem 99.9%) and high-surface-area CeO_2 (Daiichi, 99.9%, 173 $m^2\,g^{-1}$ and average particle size 46 nm; information provided by the supplier).

The catalyst was prepared by slurrying $Au(CH_3)_2(acac)$ in *n*-pentane with CeO_2 powder that had been partially dehydroxylated under vacuum at 673 K. The slurry was stirred for 24 h, and the solvent was removed by evacuation for 24 h. The resulting sample was then stored in a glove box.

2.2. Catalytic reaction experiments: oxidation of CO

All gases used in the flow reactor experiments were passed through a zeolite 4A and copper oxide trap to remove traces of moisture and O_2. A tubular quartz reactor (i.d., 0.8 cm) was used for the catalysis experiments; the reactor had a glass frit to hold the catalyst powder mixture to give a bed approximately 5 cm deep. A total catalyst mass of 25 mg, mixed with particles of inert, nonporous α-Al_2O_3, was used in each experiment.

2.3. Catalyst testing and determination of kinetics of CO oxidation

Before testing, the catalyst was treated in flowing helium at 353 ± 0.5 K for 2 h; the total gas flow rate was 200 mL(NPT) min^{-1}. After this treatment, the flow of CO and O_2 was started, and the catalyst was kept on stream for 48 h. The feed partial pressures of CO and O_2 were 1.0 kPa each, with the balance helium and the pressure atmospheric. The reactor was then cooled to 303 ± 0.5 K, and the temperature was held at this value as CO oxidation catalysis occurred; this part of the experiment also was carried out for 48 h. In preliminary experiments, we found that O_2:CO molar ratios should be kept at values exceeding the stoichiometric value of 1; otherwise, the catalyst underwent deactivation. This criterion was met in all of the kinetics experiments. Details of the effect of excess CO in the feed stream are given below.

Details of the experiments are included in the Supplemental Information, including descriptions of the sequence of steps followed for CO oxidation catalysis. The tables in the Supplemental information include details of the kinetic experiments conducted to determine the effects CO and O_2 partial pressures on the reaction rate and experiments done to investigate the effect of CO_2 introduced into the reactant feed on the reaction rate. These tables include all of the segments in each set of experiments, with the experiments numbered consecutively in the order in which they were performed.

Each measurement of a conversion was followed by an experiment carried out under standard conditions to test for catalyst stability: a total flow rate of 200 mL(NPT) min^{-1} and partial pressures of CO and O_2 of 1.0 kPa; the standard reaction temperature was 303 K. Kinetics experiments were carried out with the sample at 303 K under atmospheric pressure; the catalyst mass was 25 mg, and the total feed flow rate was 180 mL(NTP) min^{-1}. Temperature was controlled within ± 0.5 K. Conversions were always kept below 10% and were considered differential. The reactor was well approximated as an isothermal plug–flow reactor. The only product detected by gas chromatography and by mass spectrometry was CO_2. Blank experiments were done with calcined CeO_2 lacking gold under the same reaction conditions, and no conversion was observed. This finding confirms the inference that the gold was necessary for catalysis.

The feed O_2 partial pressure was varied from 1.0 to 4.6 kPa with the CO partial pressure held constant at 1.0 kPa (Table S1, Supplemental Information). The CO partial pressure was varied from 1.0 to 3.6 kPa with the O_2 partial pressure held constant at 1.0 kPa (Table S1, Supplemental Information). CO_2 was added to the feed (at partial pressures between 0.3 and 1.4 kPa), with the feed CO and O_2 partial pressures held constant at 1.1 kPa (Table S2, Supplemental Information).

The catalyst was kept on stream for at least 10 h in each segment of the kinetics experiments, and steady state was achieved in each, as confirmed by the reproducibility of the conversions (varying by only $\pm 3\%$ or less). TOF values were calculated by using steady-state conversions and the total gold content in the catalyst, with the assumption that each Au atom was accessible (as justified below on the basis of EXAFS data) [19]. Our calculations ignore the possible lack of accessibility of Au atoms at the metal–support interface.

2.4. Effect of temperature on rate of CO oxidation catalysis

CO oxidation catalysis was carried out at 333–348 K with the as-prepared catalyst as loaded into the reactor. Attainment of steady state was confirmed by essentially constant differential conversions ($<10\%$) as a function of time on stream. Similarly, the catalyst sample used for CO oxidation for 48 h at 353 and 303 K (so that gold clusters formed from the mononuclear complexes) and was tested at 303–333 K.

3. Results

3.1. Catalyst activation and attainment of steady-state operation in the flow reactor

The initially prepared sample was characterized initially by a room-temperature activity that was too low to measure with our

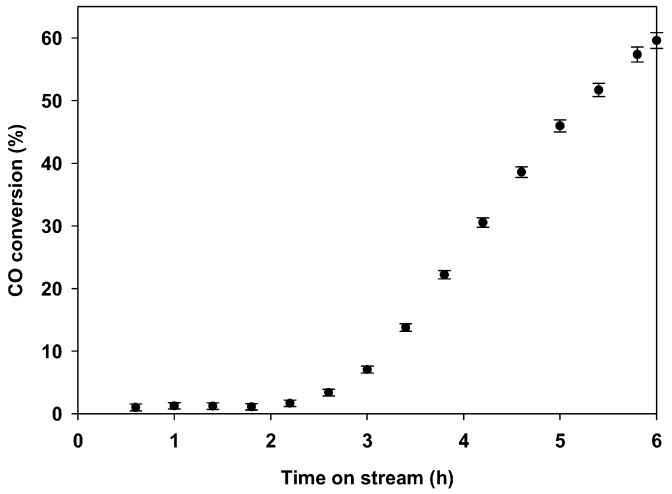

Fig. 1. Activation of gold supported on CeO_2 for CO oxidation at 353 K. Conversions were determined by gas chromatography. Total flow rate was 100 mL(NTP) min^{-1} with partial pressures of CO and O_2 of 1.0 kPa each. The catalyst mass was 25 mg; it contained 1.0 wt% Au. Conversions and TOF values were recorded during the initial 2-h period for the catalyst containing mononuclear gold species, and separately for catalyst used for periods longer than 96 h after stabilization.

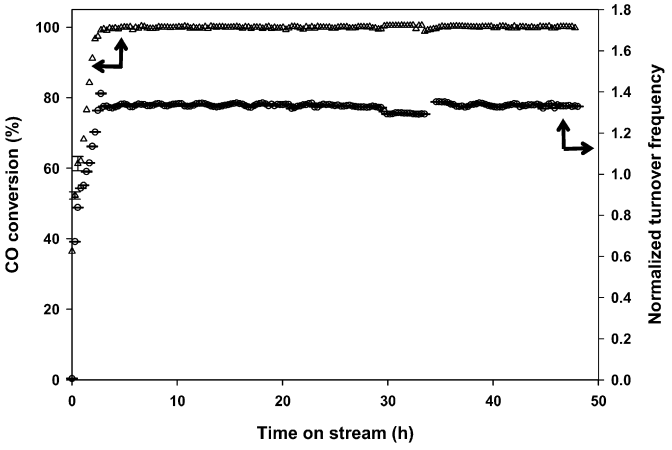

Fig. 2. Attainment of steady state in CO oxidation at 353 K. $P_{CO} = P_{O_2} = 1.0$ kPa. The as-prepared sample was treated in flowing helium for 2 h at 353 K prior to collection of the data shown here.

apparatus, but after treatment in flowing helium at 353 K for 2 h, the catalyst had a measurable activity at 353 K at feed partial pressures of $P_{CO} = P_{O_2} = 1.0$ kPa. Conversions <5% were detected (e.g., Fig. 1), corresponding to a TOF of 6.3×10^{-3} molecules of CO (Au atom s)$^{-1}$. The catalyst was stable for a sufficiently long period under these conditions to allow measurement of the reaction rate at several temperatures (data presented in Section 3.3), but the activity increased substantially as the run proceeded (Fig. 1), making measurements of the dependence of TOF on the reactant partial pressures infeasible. Thereafter, when the temperature was lowered to room temperature, catalyst activity was easily measured and increased with continuing operation in the flow reactor [19].

The conditions were subsequently modified to attain stable operation and allow kinetics measurements with the activated catalyst. At a feed flow rate higher than that corresponding to Fig. 1 (i.e., 200 mL(NTP) min^{-1} vs. 100 mL(NTP) min^{-1}), catalyst activation was more rapid, with stable operation achieved after an induction period of just a few hours (Fig. 2). Continued stable operation was observed when the temperature was lowered to 303 K (Fig. 3). The conversion versus time-on-stream data (Fig. 3) demonstrate that the conversion attained a near steady-state value of

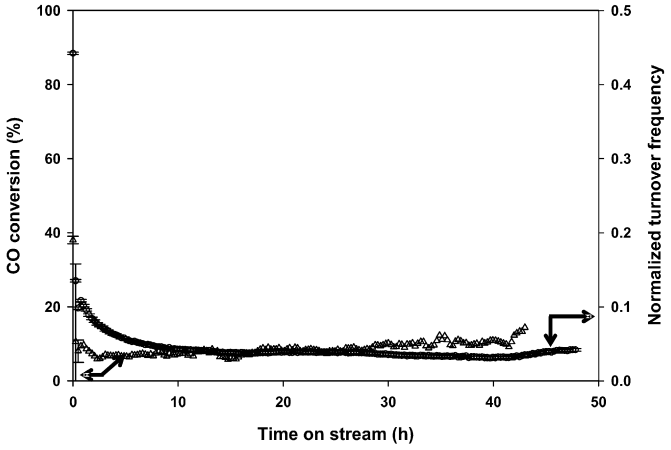

Fig. 3. Stabilization of Au/CeO_2 after activation during CO oxidation catalysis at 353 K. The data were determined for CO oxidation at 303 K with $P_{CO} = P_{O_2} = 1.0$ kPa after 48 h of operation at 353 K. Details of the experiments prior to those in which these data were determined are shown in Supplemental Information.

approximately 8% after approximately 40 h, and the corresponding TOF under these conditions was $(5.6 \pm 0.2) \times 10^{-2}$ molecules of CO (Au atom s)$^{-1}$.

An important point is that the catalyst thus stabilized afforded the opportunity for measurement of kinetics of the CO oxidation reaction. The sample used in these experiments had functioned as a catalyst for a total of 96 h.

Details of the experiments during the 96-h period and during the subsequent operation when the kinetics was measured are given in Supplemental Information Tables S1 and S2. The activity after this 96-h interval, measured under standard conditions (200 mL(NPT) min^{-1}, $P_{CO} = P_{O_2} = 1.0$ kPa, 303 K), was used as a reference in subsequent experiments to determine catalyst stability, after reaction rates from conversions determined under each set of conditions were measured. Thus, for example, after the catalyst had been tested at particular values of the partial pressures of CO, O_2, and CO_2 (Supplemental Information), it was tested for another 2 h under the standard conditions before a subsequent change in conditions, to determine further rates for establishment of the kinetics.

3.2. Determination of kinetics of CO oxidation in presence of activated catalyst

To investigate the effect of the O_2 partial pressure on the rate, the partial pressure of CO was held constant at 1.0 kPa as the partial pressure of O_2 was varied between 1.0 and 4.6 kPa. To investigate the effect of the CO partial pressure on the rate, the partial pressure of O_2 was held constant at 1.0 kPa as the CO partial pressure was varied between 1.0 and 3.6 kPa. To investigate the effect of CO_2 added to the feed on the reaction rate, the CO and O_2 partial pressures were held constant at 1.1 kPa, and the feed CO_2 partial pressure was varied between 0.3 and 1.1 kPa. In all cases, each segment for determination of a rate lasted 10 h.

The catalyst was stable under standard conditions after each segment in which the effect of O_2 partial pressure or CO_2 partial pressure was investigated. But in later experiments, when the CO partial pressure was varied, the catalytic activity decreased with time on stream. Details are presented below.

3.2.1. Effect of O_2 partial pressure on rate

The catalytic activity under standard conditions remained essentially unchanged with time on stream as the CO partial pressure was held constant and the O_2 partial pressure was varied, with fluctuations in the rates of about ±3%. The dependence of rate

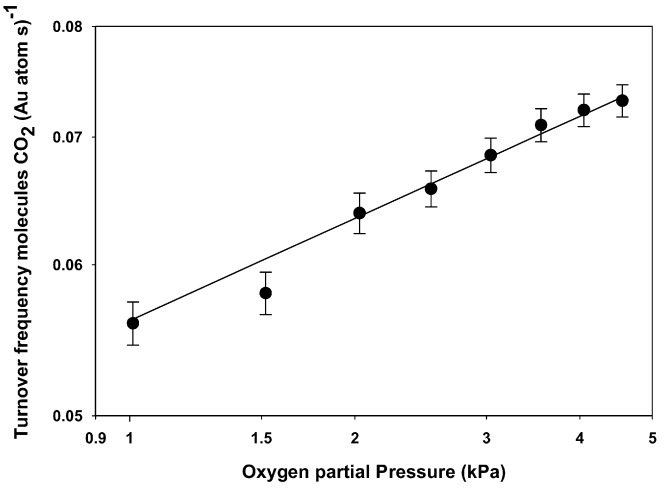

Fig. 4. Power-law kinetics of CO oxidation catalyzed by Au/CeO_2 at 303 K. $P_{CO} = 1.0$ kPa; only P_{O_2} was varied. The data show that the rate was proportional to $P_{O_2}^{0.18}$. The line corresponds to the prediction of Eq. (1), with the parameter values stated in the text. The coordinates are logarithmic.

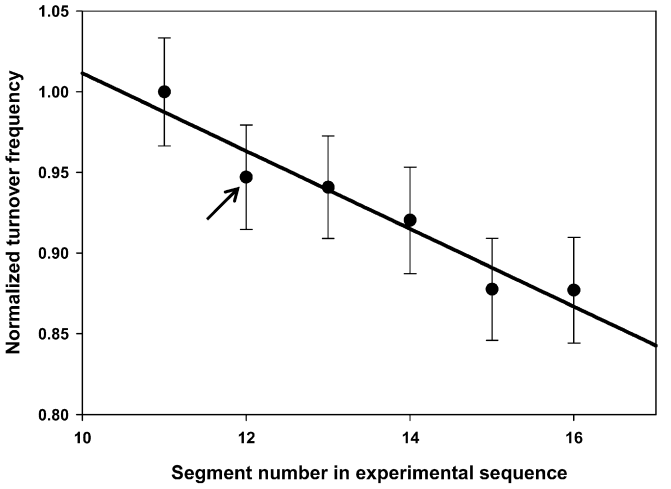

Fig. 5. Catalytic activity of Au/CeO_2 under standard conditions ($P_{CO} = P_{O_2} = 1.0$ kPa, 303 K) after variation of CO partial pressure in a sequence of increasing values. The horizontal axis represents the segment number in the experimental sequence (for details, see Supplemental Information). The sequence in which the measurements were made included an increase in CO partial pressure from one experiment to the next. The values of TOF were normalized with respect to the initial value, namely, $(5.6 \pm 0.2) \times 10^{-2}$ molecules of CO (Au atom s)$^{-1}$. The complete set of information is included in Supplemental Information.

on O_2 partial pressure is shown in Fig. 4; these TOF values were used to estimate the reaction order in O_2 (0.18), as described below (Fig. 4).

3.2.2. Effect of CO partial pressure on rate

Various values of CO partial pressures were applied in a set of experiments, summarized in detail in Table S1 in Supplemental Information. After each experiment in the series in which the CO partial pressure was varied (with the O_2 partial pressure held at 1.0 kPa), the catalyst was retested under the standard conditions (200 mL(NPT) min^{-1}, $P_{CO} = P_{O_2} = 1.0$ kPa, 303 K) to check its stability. The results demonstrate that the catalyst lost activity from one experiment to the next (Fig. 5). A typical decrease in the TOF between rechecks of the activity was 8%–10%. The catalyst underwent deactivation at all of the CO partial pressures applied in this set of experiments (i.e., $P_{CO} > 1.0$ kPa) (Fig. 5).

Thus, to estimate the influence of the CO partial pressure on the rate of the reaction in the presence of the undeactivated catalyst,

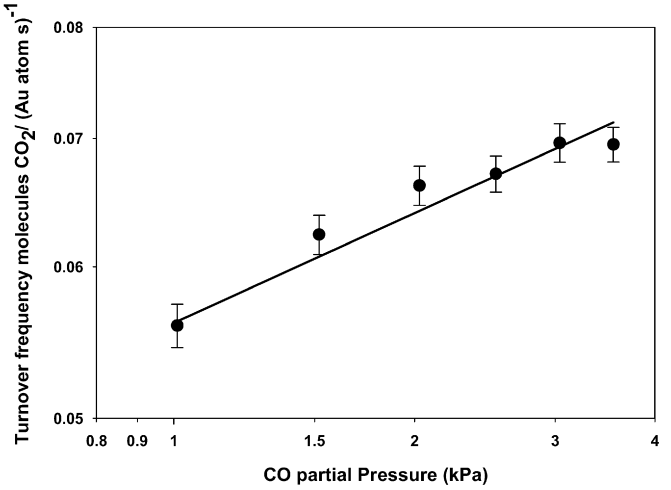

Fig. 6. Power-law kinetics of CO oxidation catalyzed by Au/CeO_2 at 303 K. $P_{O_2} = 1.0$ kPa; only P_{CO} was varied. The data were corrected to compensate for catalyst deactivation, as described in the text. They show that the reaction rate was proportional to $P_{CO}^{0.19}$. The line corresponds to the prediction of Eq. (1), with the parameter values stated in the text. The coordinates are logarithmic.

the observed TOF values were corrected to values representative of the catalyst before deactivation (and after the reaction order in O_2 had been determined). The data shown in Fig. 5 indicate how the catalyst lost activity in this set of experiments. These data represent the activity under standard conditions measured after each TOF measurement at a different CO partial pressure. With these data, each measured value of the TOF was corrected to provide an estimated value for the undeactivated catalyst. For example, the point denoted by an arrow in Fig. 5 shows that the catalyst activity was 0.88 of that at the start of this set of experiments; consequently, the TOF measured in this experiment was multiplied by 1/0.88 to determine the value used in the determination of the kinetics. These corrected TOF values were then used to estimate the reaction order in CO, 0.19, as described below (Fig. 6).

3.2.3. Effect of CO_2 partial pressure on rate

CO_2 was added to the feed stream to allow a determination of its influence on the reaction rate. These experiments were carried out with a separate batch of catalyst, so they were not influenced by the deactivation occurring during the determination of the reaction order in CO. The catalytic activity decreased with increasing CO_2 partial pressure in the feed. After each measurement of conversion, the catalyst was tested under standard conditions. No significant changes in the activity were observed, indicating that CO_2 did not cause an irreversible deactivation of the catalyst under our conditions, as might have been expected if it had led to carbonate formation, for example [9]. The order of reaction in CO_2 was found to be −0.4(4) (Fig. 7).

3.3. Summary of kinetics

In summary, the kinetics of CO oxidation catalyzed by the activated form of the supported gold is represented by the following equation, when no CO_2 is present:

$$r = k P_{CO}^{0.19} P_{O_2}^{0.18}. \quad (1)$$

When the rate (TOF) is given in units of molecules of CO converted (Au atom s)$^{-1}$, the value of k determined by the data recorded at 303 K (without CO_2 in the feed) is 5.6×10^{-2} molecules (Au atom s kPa$^{-0.37}$). The values of the parameters k and the reaction orders were determined by standard nonlinear regression of all of the data determined as described above with the CO and

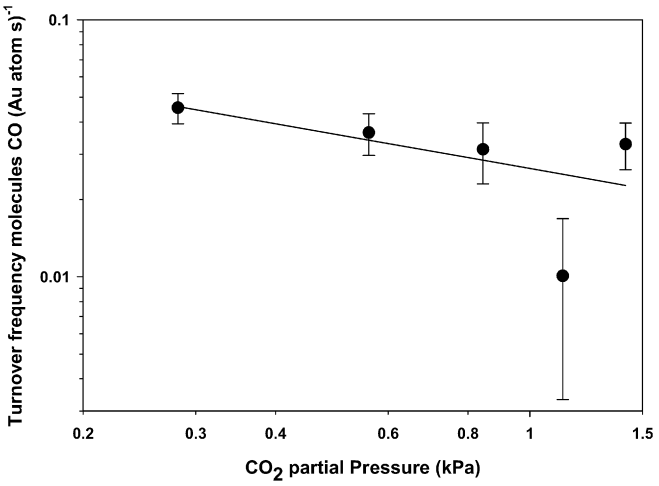

Fig. 7. Inhibition by CO_2 of CO oxidation catalyzed by Au/CeO_2 at 303 K. $P_{O_2} = P_{CO} = 1.0$ kPa, only P_{CO_2} was varied. Consideration of all the data leads to the inference that the rate was proportional to $P_{CO_2}^{-0.44}$. The line corresponds to the prediction of Eq. (2), with the parameter values stated in the text. The coordinates are logarithmic. The data point at $P_{CO_2} = 1.1$ kPa is characterized by a substantially greater error than the other data points, because of erratic operation of the gas chromatograph during this experiment. When this point is excluded from the analysis, the reaction order in CO_2 is calculated to be −0.24.

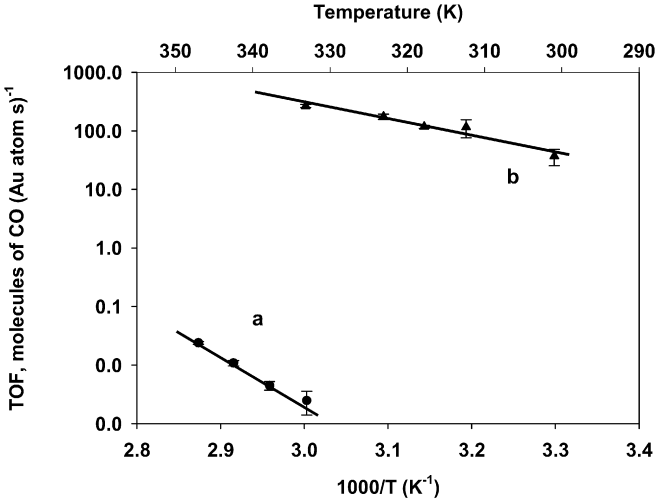

Fig. 8. Arrhenius plot (a) characterizing CO oxidation by catalyst in which gold was present as mononuclear species, as indicated by EXAFS spectroscopy. Total feed flow rate: 100 mL(NPT) min^{-1}; $P_{CO} = 1.0$ kPa, $P_{O_2} = 0.5$ kPa. For comparison (b), data are shown for the catalyst that had been activated by 48 h of operation in the flow reactor at 353 K followed by 48 h at 303 K, during which the gold aggregated to form clusters. Total feed flow rate in each experiment was 200 mL(NPT) min^{-1}; $P_{CO} = P_{O_2} = 1.0$ kPa. Conversions were <10% and thus considered differential, determining values of TOF. T is temperature.

O_2 partial pressures varied and no CO_2 present in the feed. Figs. 4 and 6 show the goodness of fit of the data with this equation.

In a similar manner, the kinetics representing the influence of CO_2 on the rate was determined from the data determined with the partial pressure of CO_2 varied and the partial pressures of CO and O_2 fixed. To determine the value of k' and the order of reaction in CO_2, the values of the reaction orders in CO and in O_2 determined as stated above were fixed. The following equation represents the data:

$$r = k' P_{CO}^{0.19} P_{O_2}^{0.18} P_{CO_2}^{-0.44}. \quad (2)$$

When the rate (TOF) is given in units of molecules of CO converted (Au atom s)$^{-1}$, the value of k' determined by the data recorded at 303 K is 2.6×10^{-2} molecules (Au atom s $kPa^{0.07}$). The goodness of fit of the data with this equation is shown in Fig. 7. The precision with which the reaction order in CO_2 was determined is clearly less than that characterizing the reaction orders in CO and in O_2 (Fig. 7); thus, we are less confident in the appropriateness of power-law kinetics to represent the inhibition by CO_2.

3.4. Effect of temperature on rate of CO oxidation

The temperature dependence of the rate of reaction catalyzed by the as-prepared sample is shown in the Arrhenius plot of Fig. 8. The apparent activation energy is 138 ± 2 kJ mol^{-1}. The data characterizing the activated catalyst are also shown. The apparent activation energy is 54 ± 8 kJ mol^{-1}. These data thus clearly show that the two forms of the catalyst have markedly different performance characteristics.

4. Discussion

The data presented in Figs. 1 and 2 show that operation of the catalyst in the flow reactor led to a marked increase in its activity. In work that has been communicated [19], we showed that the catalyst initially was characterized by an extended X-ray absorption fine structure (EXAFS) spectrum and an X-ray absorption near edge structure (XANES) spectrum consistent with the presence of mononuclear (single-gold-atom) complexes, with gold in an oxidation state of approximately +3 [19,20]. There was no EXAFS evidence of gold clusters in the sample. This result is similar to results characterizing catalysts made from the same precursor ($Au(CH_3)_2(acac)$) on various supports [20,21].

Reports of cationic gold complexes on supports indicate that they are active for CO oxidation catalysis [22,23], but the activities are low relative to those of some catalysts that incorporate gold clusters on supports. Comparisons of catalysts consisting essentially of mononuclear gold complexes on the one hand and gold clusters on the other hand have been lacking, because of difficulties in preparing samples consisting of just the one or the other catalytic species. Even when such samples can be prepared, they often are not stable, because supported gold complexes and small clusters readily undergo reduction and aggregation of the metal [24].

The results presented here fill this gap. The data, consistent with results reported previously [19], demonstrate that the catalyst initially containing supported gold complexes was sufficiently stable to allow measurements of TOF for CO oxidation, but that it gained activity during subsequent operation in a flow reactor. The XANES and EXAFS data show that as the catalyst operated in the flow reactor and gained activity, the gold was reduced and aggregated into clusters [19].

The EXAFS data characterizing the catalyst that had been used for 24 h at 353 K in the flow reactor show that it incorporated gold clusters with an average Au–Au coordination number of 4, corresponding to an average gold cluster diameter of about 4 Å. The sample containing these small clusters is characterized by a XANES spectrum between those spectra characterizing gold cations on the support and gold foil (or gold particles on the support). Thus, we infer that the gold was not entirely metallic in the sample incorporating the slightly aggregated gold.

The catalyst that had been kept on stream for a longer period (48 h) attained stable activity (Fig. 2). EXAFS results characterizing a catalyst used under almost the same conditions for the same period [19] show that it contained gold clusters consisting of approximately 15 atoms each on average, with a diameter of roughly 9 Å (presuming spherical clusters). The XANES spectrum of this sample was quite similar to that of metallic gold [19]. Thus, we infer that during operation in the flow reactor, the gold in our catalyst had undergone aggregation into clusters as it was reduced to nearly the zero-valent state.

Table 1
Comparison of activities of supported gold catalysts for CO oxidation at atmospheric pressure.

Catalyst	Approximate average gold cluster diameter (Å)	Time on stream (h)[a]	T (K)	Approximate TOF/molecules of CO converted (Au atom s)$^{-1}$	Partial pressure of CO/O_2/CO_2 (kPa)	Ref.
Au/CeO_2 (initially)	[b]	2.5	353	6.5×10^{-3}	1.0/1.0/0	This work
Au/CeO_2 (after activation)	4	50	353	[c]	1.0/1.0/0	This work
Au/CeO_2 (activated)	7	68[d]	298	$>3.2 \times 10^{-2}$	1.0/1.0/0	This work
Au/CeO_2 (stabilized)	7	96[e]	303	5.6×10^{-2}	1.0/1.0/0	This work
Au/La_2O_3	[b]	50	298	1.2×10^{-2}	1.6/1.6/0	[21]
Au/CeO_{2-x}	40	10	278	2×10^{-2}	0.2/20/0	[13]
Au/zeolite NaY	[b]	1	298	3×10^{-3}	1.6/1.6/0	[22]
Au/Al_2O_3	24	>0.5	273	3×10^{-2}	1.6/1.6/0	[27]
Au/Fe_2O_3	<10	10	293	[c]	0.9/92/0	[31]
Au/TiO_2	40	Not stated	282	3.4×10^{-2}	1.0/21.1/0	[7]
Au/TiO_2	300	Not stated	313	1.3×10^{-3}	5.0/5.0/0	[8]
Au/Fe_2O_3	20–37	Not stated	353	1.3×10^{-3}	0.9/92/0	[32]

[a] Time corresponds to the time the catalyst was on stream under the conditions specified.
[b] Undetectable from EXAFS spectroscopy.
[c] Cannot be calculated because conversions exceeded differential.
[d] Time of operation in CO oxidation at 298 K after 50 h of operation in CO oxidation at 353 K.
[e] Catalyst after two periods of operation of 48 h each, the first at 353 K followed by a second at 303 K.

The central finding of this work is that the catalyst in which the gold was present as mononuclear complexes (in the absence of detectable gold clusters) was active, and the catalyst in which gold clusters formed was more active. The marked difference in the activities of the catalysts before and after activation demonstrates that the gold complexes and gold clusters were active separately.

Comparing the apparent activation energies of the two forms of the catalyst (Fig. 8) reinforces the contrast between them. The apparent activation energies differ by a factor of approximately 3 (Fig. 8). These findings strongly suggest that the mechanism of CO oxidation on the catalyst incorporating the mononuclear gold differs from that on the catalyst incorporating the clusters. The result weighs against the possibility that the catalysis observed with the sample incorporating the mononuclear gold complexes should be attributed to undetected gold clusters rather than to the complexes themselves.

It is becoming increasingly clear [25] that CO oxidation is not a highly informative test reaction for characterization of supported gold catalysts; evidently, the reaction is facile and may occur via multiple mechanisms. Thus, we infer that it may not be fruitful to consider it likely that any of the reaction mechanisms proposed for CO oxidation on gold [e.g., 7,8,26] may be general.

Although the X-ray absorption spectra indicate that the gold in our activated catalyst is largely zero-valent, IR spectroscopy has provided some evidence suggesting that matters may not be so simple. The data of Mihaylov et al. [27] characterizing gold on La_2O_3 in the presence of CO and in the presence of CO_2 provide evidence of facile redox processes involving gold highly dispersed on oxide supports. The reduction of the Au(III) complexes in the $CO + O_2$ reaction mixture is explained by autoreduction of the gold. Furthermore, however, Mihaylov's IR data [27] show that the process can be reversed in CO_2—essentially zero-valent gold in supported clusters can be oxidized by CO_2.

Thus, these results point to the possibility that both zero-valent and cationic gold may exist in the working catalysts. Some authors [28] have speculated that cationic gold at the gold–support interface may be present and help to stabilize the gold clusters, and that it also might participate in the catalytic reaction. Recent work by Herzing et al. [29] presented X-ray photoelectron spectra suggesting both cationic and zero-valent gold supported on iron oxide. These authors used aberration-corrected scanning transmission electron microscopy to detect gold species ranging from individual gold atoms (which we would expect to be stable only as cations) and clusters with diameters of 0.2–0.5 nm, along with some substantially larger clusters. The observations led them to propose an important role of gold clusters with diameters in the range of 0.2–0.5 nm in CO oxidation catalysis. The sizes of these clusters are not much different from ours, but their sample likely was characterized by a much wider range of cluster sizes.

The results presented here are broadly consistent with the literature of gold catalysts in showing that the support has a significant influence on the activity for CO oxidation [30] (as well as other reactions). The results indicating activity of supported mononuclear gold complexes demonstrate a strong support effect [21,22]. Our findings indicate that CeO_2 as a support gives a mononuclear gold catalyst that is substantially less active than the most active supported mononuclear gold catalysts reported to date (Table 1).

Table 1 provides a comparison of the activities of our catalyst in both forms with those of some similar supported gold catalysts for CO oxidation. We caution that comparisons of the reported activities of these catalysts are not straightforward, because the catalyst synthesis methods, supports, and reaction conditions are not the same, and details often are not reported. There have been only a limited number of reports of turnover frequencies (as summarized in Table 1), and hardly any reports of reaction kinetics.

Power law equations have been used to represent the kinetics [7,8], and we found this representation to be appropriate for our data as well. We stress that our catalyst was stable in operation in the flow reactor only when O_2 was in stoichiometric excess over CO, and thus the rate equation (1) is limited to that composition range and does not account for the inhibition by CO_2, which is accounted for by Eq. (2), which is valid only for the range of CO_2 partial pressures investigated. The low orders of reaction in the reactants CO and O_2 (0.19 and 0.18, respectively) are broadly in agreement with (the few) values reported for supported gold catalysts [8,31].

The data do not indicate why our catalyst underwent rapid deactivation when CO was present in a stoichiometric excess. Various explanations of the deactivation of supported gold catalysts for CO oxidation have been offered, including the effects of gold cluster size [33] and oxidation state [14] and the influence of chlorine from the catalyst precursor (typically, $HAuCl_4$ and $AuCl_3$) [8]. Some authors have suggested the blocking of catalytic sites by carbonates (or related species such as formates) formed from CO or CO_2 on the catalyst [9,11].

Consequently, the role of CO_2 as a reaction inhibitor observed in our work (and similarly by Hoflund et al. [29]) might indicate the formation of carbonates or related species on the gold, deactivating the catalyst in the experiments in which CO was present in excess in the feed. We rule out this possibility, however, because the effect of CO_2 was reversible, meaning that soon after CO_2 was removed from the feed, the catalytic activity returned to its origi-

nal value. Thus, the results suggest rather weak, reversible bonding of CO_2 or species formed from it to the catalytic sites (or nearby sites).

Although the mechanism of CO oxidation on our catalyst is poorly understood, we can infer from the kinetics that both CO and O_2 were adsorbed. The similar (and small) values of the reaction orders in CO and O_2 (0.19 and 0.18, respectively) suggest that both reactants were bonded to the gold and that neither reactant dominated nor covered most of the surface.

The full role of CeO_2 in the reaction remains to be elucidated, but it is clear that the surface chemistry of this support is important in the catalysis [3,16]. Raman spectra [16,34] show that among the various oxygen species that are formed on the CeO_2 surface, some are highly reactive; η^1-superoxide and peroxide adspecies have been suggested to be involved as intermediates in the CO oxidation reaction [16].

5. Conclusion

In this work, $Au(CH_3)_2(acac)$ was used to synthesize mononuclear cationic gold complexes on CeO_2. These are active for CO oxidation catalysis, and during operation in a flow reactor, the gold is reduced and aggregated into small clusters (approximately 9 Å in diameter), which are much more active than the mononuclear species and are characterized by an apparent activation energy of 54 $kJ\,mol^{-1}$, only about one-third of the value characterizing the supported gold complexes. The CO oxidation reaction catalyzed by the supported gold clusters is characterized by orders of reaction of 0.19 in CO, 0.18 in O_2, and -0.4 in CO_2.

Acknowledgments

This research was supported by the Department of Energy (FG02-04ER15513) and CONACyT (175763 VAG). We acknowledge the National Synchrotron Light Source, beam line X-18B, and the Stanford Synchrotron Radiation Laboratory, beam line 2–3, for beam time. We thank the beam line staffs for their assistance.

Supplemental Information

The online version of this article contains additional supplemental information.

Please visit DOI: 10.1016/j.jcat.2008.09.012.

References

[1] G.J. Hutchings, Catal. Today 100 (2005) 55.
[2] M. Haruta, T. Kobayashi, H. Sano, N. Yamada, Chem. Lett. (1987) 405.
[3] W. Deng, A.I. Frenkel, R. Si, M. Flytzani-Stephanopoulos, J. Phys. Chem. C 112 (2008) 12834.
[4] S. Hashmi, G.J. Hutchings, Angew. Chem. Int. Ed. 45 (2006) 7896.
[5] M. Mihaylov, H. Knözinger, K. Hadjiivanov, B.C. Gates, Chem. Ing. Tech. 79 (2007) 795.
[6] M. Haruta, CATTECH 6 (2002) 102.
[7] G.R. Bamwenda, S. Tsubota, T. Nakamura, M. Haruta, Catal. Lett. 44 (1997) 83.
[8] (a) S.D. Lin, M. Bollinger, M.A. Vannice, Catal. Lett. 17 (1993) 245; (b) M.A. Bollinger, M.A. Vannice, Appl. Catal. B 8 (1996) 417.
[9] (a) B. Chang, B.W. Jang, S. Dai, S.H. Overbury, J. Catal. 236 (2005) 392; (b) J.C. Clark, S. Dai, S.H. Overbury, Catal. Today 126 (2007) 135.
[10] J.T. Calla, R.J. Davis, J. Catal. 241 (2006) 407.
[11] G.B. Hoflund, S.D. Gardner, Langmuir 11 (1995) 3431.
[12] Y. Denkwitz, Z. Zhao, U. Hörmann, U. Kaiser, V. Plzak, R.J. Behm, J. Catal. 251 (2007) 363.
[13] S. Carrettin, P. Concepción, A. Corma, J.M. Lopez Nieto, V.F. Puntes, Angew. Chem. Int. Ed. 43 (2004) 2538.
[14] J. Guzman, B.C. Gates, J. Phys. Chem. B 107 (2003) 2242.
[15] M. Daté, M. Okumura, S. Tsubota, M. Haruta, Angew. Chem. Int. Ed. 43 (2004) 179.
[16] J. Guzman, S. Carretin, J.C. Fierro-Gonzalez, Y. Hao, B.C. Gates, A. Corma, Angew. Chem. Int. Ed. 44 (2005) 4778.
[17] J. Guzman, S. Carretin, A. Corma, J. Am. Chem. Soc. 127 (2005) 3286.
[18] J. Guzman, B.C. Gates, Langmuir 19 (2003) 3897.
[19] V. Aguilar-Guerrero, B.C. Gates, Chem. Commun. (2007) 3210.
[20] J. Guzman, B.C. Gates, J. Catal. 224 (2004) 111.
[21] J.C. Fierro-Gonzalez, V.A. Bhirud, B.C. Gates, Chem. Commun. (2005) 5275.
[22] J.C. Fierro-Gonzalez, B.C. Gates, J. Phys. Chem. B 44 (2004) 16999.
[23] J. Guzman, J.C. Fierro-Gonzalez, V. Aguilar-Guerrero, Y. Hao, B.C. Gates, Z. Phys. Chem. 219 (2005) 921.
[24] J.C. Fierro-Gonzalez, B.C. Gates, J. Phys. Chem. B 109 (2005) 7275.
[25] J.C. Fierro-Gonzalez, B.C. Gates, Catal. Today 122 (2007) 201.
[26] C.K. Costello, J.H. Yang, H.Y. Law, Y. Wang, J. Lin, L.D. Marks, M.C. Kung, H.H. Kung, Appl. Catal. A 243 (2003) 15.
[27] M. Mihaylov, E. Ivanova, Y. Hao, K. Hadjiivanov, B.C. Gates, H. Knözinger, Chem. Commun. (2008) 175.
[28] G.C. Bond, D.T. Thompson, Catal. Rev.-Sci. Eng. 91 (1999) 319.
[29] A.A. Herzing, C.J. Kiely, A.F. Carley, P. Landon, G.J. Hutchings, Science 321 (2008) 1331.
[30] M. Haruta, Catal. Today 36 (1997) 153.
[31] N.A. Hodge, C.J. Kiely, R. Whyman, M.R. Siddiqui, G.J. Hutchings, Q.A. Pankhurst, F.E. Wagner, R.P. Rajaram, S.E. Golunski, Catal. Today 72 (2002) 133.
[32] M.M. Schubert, S. Hackenberg, A.C. van Veen, M. Muhler, V. Plzak, R.J. Behm, J. Catal. 197 (2001) 113.
[33] M. Haruta, J. New Mat. Electrochem. Syst. 7 (2004) 163.
[34] V.V. Pushkarev, V.I. Kovalchuk, J.L. d'Itri, J. Phys. Chem. B 108 (2004) 5341.